Rare Metal Materials and Engineering
Volume 49, Issue 11, November 2020
Available online at www.rmme.ac.cn

Science Press

Cite this article as: Rare Metal Materials and Engineering, 2020, 49(11): 3724-3733.

ARTICLE

Numerical Simulation and Experimental Research of Magnesium Alloy Plate Asymmetrical Rolling

Wang Xi, Xue Zhengkun, Yu Xiaoguang, Yang Youze

School of Mechanical Engineering and Automation, University of Science and Technology Liaoning, Anshan 114051, China

Abstract: The effects of different process parameters on the properties of the products of unidirectional asynchronous rolling of magnesium alloy plate were analyzed using numerical simulation technique and experimental study. ANSYS/LS-DYNA finite element software was also used to complete the numerical simulation and the experimental study of unidirectional asynchronous rolling was carried out under different rolling conditions. Besides, the internal structure was observed by metallographic microscope, and the yield strength, tensile strength and hardness of the magnesium alloy plate were tested by tensile testing machine and micro Vickers hardness tester.

Key words: magnesium alloy plate; asymmetrical rolling; numerical simulation; metallographic microstructure; uniaxial tension

Since its discovery nearly two centuries ago, magnesium has been rapidly and widely used for its unique advantages of light mass, high specific strength, good rigidity and large damping capacity, excellent shock absorption, thermal conductivity and electromagnetic compatibility[1,2]. Magnesium alloys were first used in the industrial field by German in 1886, and it was not until the mid-1990s that the application of magnesium alloys became mature. In recent years, due to its outstanding performance incomparable with other metal materials, magnesium alloy has been increasingly applied in automobile transportation, 3C products and other fields. It is also known as "green engineering material of the 21st century"[3,4].

At present, the research on the plastic processing technology of magnesium and its alloys has made some achievements, but there are still many problems. For example, the high viscosity, thermal conductivity and deformation temperature of magnesium alloy materials lead to high temperature requirements in stamping and forging[5.6], insufficient flow filling capacity, coarse grain and low speed[7]. In addition, the extrusion magnesium alloy forming technology has many defects, such as low material utilization rate, fast die wear, low extrusion speed, uneven product structure and strong anisotropy[8-11]. However, although rolling is the main method for the preparation of magnesium alloy plates, there are still many problems, such as the difficulty in the billet opening, the small amount of single-pass deformation, and the low yield of thin plates[12,13]. In order to solve the above problems in magnesium alloy processing, new technologies such as multi-direction forging, isothermal extrusion, ECAE and high-pressure torsion have emerged in recent years [14-16].

Although it cannot completely solve the defects of magnesium alloy processing[17,18], the method combined with the plastic deformation theory of magnesium alloy provides a new idea for the plastic forming of magnesium alloy. Through asynchronous rolling technology, the properties of magnesium alloys can be modified effectively.

1 Numerical Simulation and Result Analysis of Asynchronous Rolling of Magnesium Alloy Plate

1.1 Constitutive model setting

The elastic-plastic finite element method is used for nu-

Received date: November 24, 2019
Foundation item: Doctor's Start-up Fund of Science and Technology Department of Liaoning Province (20170520313); Education Department of Liaoning Province (2016HZPY04)
Corresponding author: Yu Xiaoguang, Ph. D., Professor, School of Mechanical Engineering and Automation, University of Science and Technology Liaoning, Anshan 114051, P. R. China, E-mail: yuxiaoguang58@163.com

merical simulation, in which the elastic stage conforms to the generalized Hooke's law, and the plastic stage conforms to the Prandtl-Reuss hypothesis, so as to deal with the relationship between stress and strain in the process of metal plastic forming.

In the elastic deformation phase of metal, the relationship between stress and strain is linear. The strain has nothing to do with the deformation process, but is only determined by and corresponding to the final stress state, which is given in the following full form:

$$\{\sigma\} = [D]_e\{\varepsilon\} \tag{1}$$

When the equivalent stress at a point in the material reaches a value irrelevant to the stress state at that point, the equivalent stress value is the yield limit, and the relationship between stress and strain is determined by the elastic-plastic matrix $[D]_{ep}$ of the material (ep represents elastic-plastic), as shown below:

$$\mathrm{d}\{\sigma\} = [D]_{ep}\,\mathrm{d}\{\varepsilon\} \tag{2}$$

By deducing Eq.(2), we can get:

$$[D]_{ep} = \frac{E}{1+v}\cdot\begin{bmatrix} \frac{1-v}{1-2v}-\omega\sigma_x'^2 & \frac{v}{1-2v}-\omega\sigma_x'\sigma_y' & \frac{v}{1-2v}-\omega\sigma_x'\sigma_s' & -\omega\sigma_x'\tau_{xy} & -\omega\sigma_x'\tau_{ys} & -\omega\sigma_x'\tau_{sx} \\ & \frac{1-v}{1-2v}-\omega\sigma_y'^2 & \frac{v}{1-2v}-\omega\sigma_y'\sigma_s' & -\omega\sigma_y'\tau_{xy} & -\omega\sigma_y'\tau_{ys} & -\omega\sigma_y'\tau_{sx} \\ & & \frac{1-v}{1-2v}-\omega\sigma_s'^2 & -\omega\sigma_s'\tau_{xy} & -\omega\sigma_s'\tau_{ys} & -\omega\sigma_s'\tau_{sx} \\ & & & \frac{1}{2}-\omega\tau_{xy}^2 & -\omega\tau_{xy}\tau_{ys} & -\omega\tau_{xy}\tau_{sx} \\ & \text{Symmetry} & & & \frac{1}{2}-\omega\tau_{ys}^2 & -\omega\tau_{ys}\tau_{sx} \\ & & & & & \frac{1}{2}-\omega\tau_{sx}^2 \end{bmatrix} \tag{3}$$

In Eq.(3):

$$\omega = \frac{9G}{2\sigma_{ij}^2(H'+3G)} \tag{4}$$

In Eq.(4) H' represents the shear elastic modulus of the material

$$H' = \frac{\mathrm{d}\sigma_i}{\mathrm{d}\varepsilon_i^p} \tag{5}$$

In Eq.(4) σ_{ij} represents the component of the stress deviator. Johnson Cook constitutive model was used in the simulation study [19].The constitutive model is as follows:

$$\sigma = [A + B\varepsilon^n][1 + c\ln(\frac{\dot{\varepsilon}}{\dot{\varepsilon}_0})][1 - (\frac{T - T_r}{T_m - T_r})^m] \tag{6}$$

Where A, B and n represent the strain strengthening term coefficients of materials; c represents the strengthening term coefficient of material strain rate; m represents the thermal softening coefficient of materials

By deducing Eq.(6), we can get: $\dot{\varepsilon}_0$ represents strain rate, T_r represents the reference temperature, T_m represents the melting point of the material.

1.2 Model establishment and parameter setting

In this paper, ANSYS/LS-DYNA is used for numerical simulation. The rolling process is asynchronous because of the different diameters of the upper and lower rolls in the rolling model. It is affected by complex factors such as large deformation, large displacement, material nonlinearity, contact nonlinearity, boundary nonlinearity and friction nonlinearity[20-22]. Therefore, the following simplification is carried out: (1) The elastic deformation of the roll is neglected in the rolling process, that is to say, it is assumed to be rigid body and the magnesium alloy plate is isotropic; (2) The temperature in the rolling process is fixed, that is to say, the influence of conduction factors on the temperature of the whole rolling process is not considered; (3) Friction between models is treated by coulomb friction, and the friction coefficients of upper and lower rolls are the same[23,24].

In this paper, when establishing the geometric model for simulation analysis, in order to improve the calculation efficiency, according to the simplification and the symmetry of the model, only 1/2 of the thin plate geometric model was taken for analysis and calculation[25], that is, the length of magnesium alloy thin plate is 100 mm, the width is 50 mm and the thickness is 2 mm. The support roll and work roll models are treated with rigid body in the rolling mill, so only the work roll model was established. The specific geometric parameters are: the diameter of the upper roll is 60 mm, and the diameter of the lower roll is 80 mm. After the establishment of the geometric solid model, both the roll and the magnesium alloy plate adopt the explicit body element solid164, which is dispersed by sweep, as shown in Fig.1.

In the numerical simulation, the average strain rate of asynchronous rolling of magnesium alloy plate is expressed by Wusatowski formula[26,27]:

$$\dot{\varepsilon} = \frac{N\pi}{30}\sqrt{\frac{R\varepsilon}{h}} \tag{7}$$

Where $\dot{\varepsilon}$ means average strain rate of magnesium alloy plate (s^{-1}); N stands for roll speed (r/min); R stands for roll radius (mm); h represents the thickness of plate after rolling (mm); ε is rolling reduction rate, expressed as a percentage.

It can be known that, when the average strain rate of

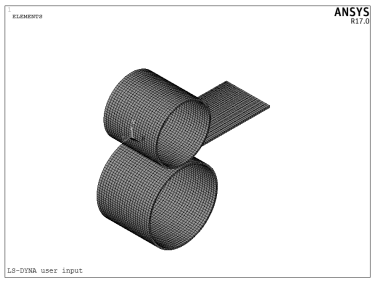

Fig.1 Asynchronous rolling unit model of AZ31B magnesium alloy

magnesium alloy thin plate is 2 s^{-1} and the roll speed is 20 r/min, the corresponding reduction is obtained, and the experiment is arranged based on this as the basic velocity condition. The rolling conditions and the basic parameters of the geometric model are shown in Table 1.

According to the parameters shown in Table 1, a basic numerical simulation model for the asynchronous rolling of magnesium alloy plate is established. It should be noted that: (1) The reduction given in Table 1[3] is only used as the basic condition of reduction; (2) although the upper and lower rolls are rotating about the *X* axis, but in the opposite direction; (3) The plate moves in the positive direction to the *Z* axis. After consulting relevant materials and literature, we obtained the material characteristics of AZ31B at 280 ºC, the specific properties of which are shown in Table 2[28].

This paper mainly discusses and studies the properties of magnesium alloy plate after asynchronous rolling at different pressure reductions. Therefore, after consulting relevant research data and verifying the feasibility, four gradients of 20%, 25%, 40% and 50% were selected for the numerical simulation of rolling reduction rate, that is, the reduction is 0.4, 0.5, 0.8 and 1 mm.

1.3 Analysis of numerical simulation results

1.3.1 Effect of rolling conditions on rolling force of magnesium alloy plate

Fig.2 shows the variation curves of rolling force on magnesium alloy plate under different reductions during the whole rolling process. In Fig.2a~2d, the rolling reduction is 0.4, 0.5, 0.8 and 1.0 mm, respectively.

First of all, as can be seen from Fig.2, during the rolling process, when the plate is first bitten, the rolling force rises rapidly. Then, when the plate is completely bitten, the rolling force tends to be stable and fluctuates up and down in a certain range. Finally, at the end of rolling, the rolling force decreases rapidly. By comparing the four curves in Fig.2a~2d, it is found that the rolling force increases with the increase of the reduction, and the fluctuation becomes more unstable. Fig.3 shows the variation curve of the maximum rolling force on the plate with the reduction rate. It can be seen from the figure that the rolling force

Table 1 Basic parameter settings of numerical simulation[3]

Mean strain rate/s^{-1}	Upper roll radius/mm	Reduction ratio/%	Thickness/ mm	Rotation speed/r·min^{-1}
2	30	25	2	20

Table 2 Performance parameters of AZ31B at 280 ºC [28]

Density/ kg·m^{-3}	Elastic modulus/MPa	Poisson's ratio	Yield stress/N	Shear modulus/MPa
1780	464.88	0.35	171.72	79.4

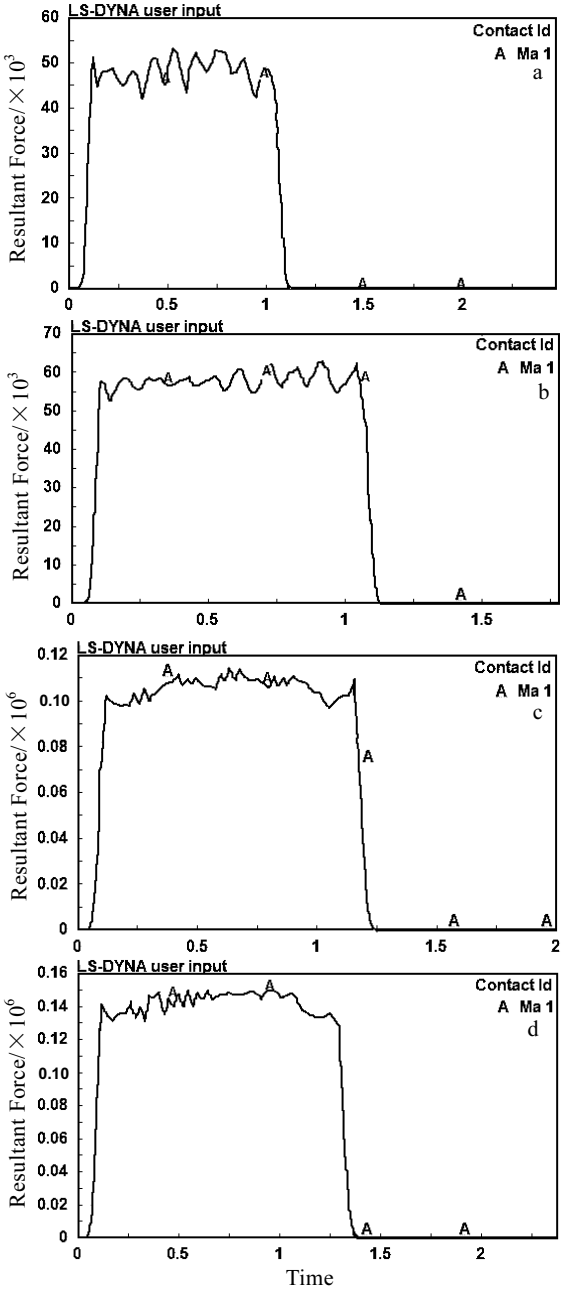

Fig.2 Rolling force variation curves under different rolling reductions: (a) 0.4 mm, (b) 0.5 mm, (c) 0.8 mm, and (d) 1.0 mm

increases with the increase of the reduction rate. When the reduction rate is large, the increase of rolling force becomes rapidly.

1.3.2 Effect of rolling reductions on equivalent stress of magnesium alloy plate

Fig.4 shows the cloud diagram of the equivalent stress distribution of the rolled magnesium alloy plate under different reductions. In Fig.4a~4d, the reduction distribution is 0.4, 0.5, 0.8 and 1.0 mm, respectively. From the observation and analysis of Fig.4, it can be seen that when the rolling is complete, the equivalent stress of the head and tail of the plate is the most concentrated, reaching the maximum value. In addition, the equivalent stress of the edge is larger than that of the middle part, and the larger the reduction is, the more obvious such phenomenon will be.

This distribution and the distribution of rolling force show obvious consistency, that is, the rolling force on the plate in the head, tail and edge are also greater than that in the middle. Therefore, the equivalent stress in the middle of the plate is relatively uniform, and the head, tail and edge of the plate are more prone to stress concentration in the rolling process.

1.3.3 Effect of rolling reductions on thickness displacement and edge deformation of magnesium alloy plate

Fig.5 show the variation curves of plate thickness displacement under different rolling reductions after the whole rolling process. Fig.5a shows the variation curve of thickness displacement on the side of fast roll, while Fig.5b shows the variation curve of thickness displacement on the side of slow roll. It can be seen from the figure that, whether on the fast side or on the slow side, the thickness displacement of the plate is relatively stable when the rolling reduction is small; when the rolling reduction is large, there is a big fluctuation. This is due to the large internal strain rate of the plate when the rolling reduction is large, which indicates that larger asynchronous rolling reduction can improve the internal structure of the plate to a certain degree; with the increase of the rolling reduction, the thickness displacement of the plate also increases, but the general trend remains the same. Fig.6 shows the variation curve of plate thickness displacement with rolling reductions.

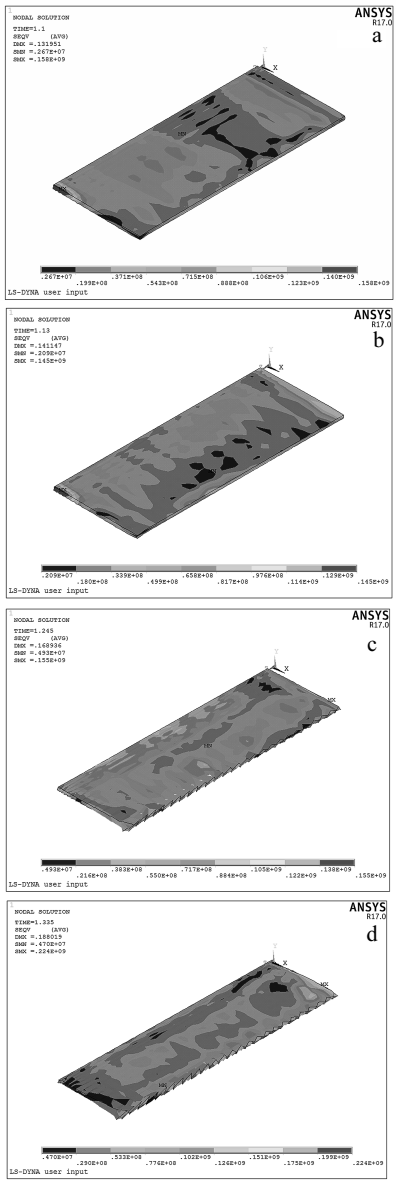

Fig.4 Cloud diagrams of equivalent stress distribution of plate fully rolled under different rolling reductions: (a) 0.4 mm, (b) 0.5 mm, (c) 0.8 mm, and (d) 1.0 mm

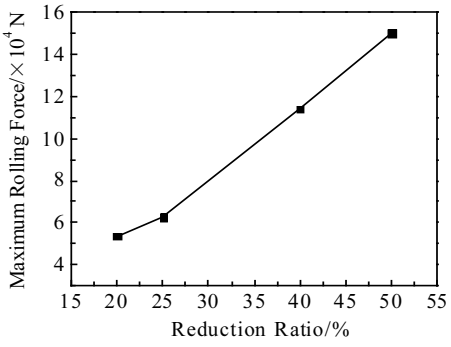

Fig.3 Variation curve of maximum rolling force with the rolling reduction ratio

Fig.7 is the cloud diagram of equivalent strain distribution of the plate fully rolled under different rolling reductions, in which the reduction of Fig.7a~7d is 0.4, 0.5, 0.8 and 1 mm, respectively. It can be seen from the figure that the equivalent strain on the edge of the plate is relatively large under each rolling reduction, and the rolling reduction has a great impact on the edge deformation of the plate. The lateral flow of edge metal will obviously increase with the increase of the rolling reduction, and the larger the re-

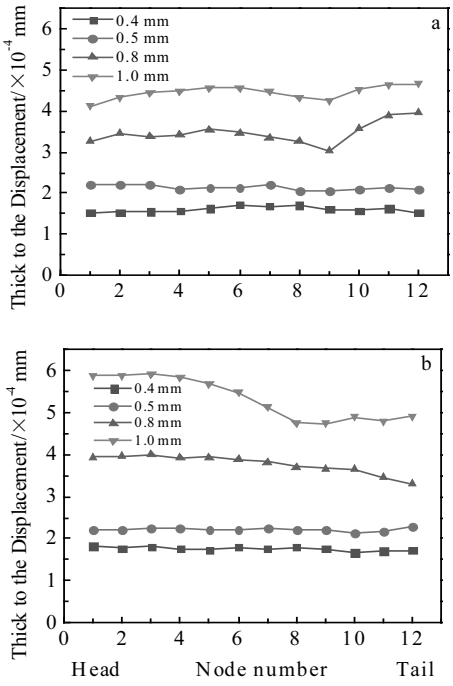

Fig.5 Variation curves of plate thickness displacement under different rolling reductions: (a) fast roll and (b) slow roll

duction is, the greater the edge deformation will be, which is the reason why edge crack is easy to occur under large rolling reduction in actual production.

As can be seen from Fig.7, the longitudinal strain at rolling is uneven and increases with the increase of the rolling reduction. Large reduction is bound to lead to a large rolling force, and large rolling force will also act on the roll, and make the roll bending, resulting in an increase of edge drop. At the same time, large equivalent strain also exists in the head and tail of the plate.

2 Asynchronous Rolling Experiment and Result Analysis

2.1 Experimental materials and research methods [29]

Experiments were designed according to the numerical simulation process of the asynchronous rolling of magnesium alloy plates. The experiments mainly studied the asynchronous rolling of magnesium alloy plates at 280 ºC. The overall research route of the experiment is as follows: before rolling, clean the surface of the plate and heat it to 280 ºC before rolling. Four groups of single pass asynchronous rolling experiments were carried out for 8 times by selecting the rolling reduction ratio as 20%, 25%, 40% and 60%, that is, the rolling reduction as 0.4, 0.5, 0.8 and 1.2 mm, respectively. After the rolling was finished, the plate was cooled naturally indoors or cooled quickly in water. By metallographic microscope analysis[30,31], the metallographic microstructure of the plates in two directions, i.e. rolling direction and width direction of each group of rolled parts were observed, and the micro Vickers hardness of the plate surface was tested. Finally, the tensile properties of the rolled magnesium alloy plate at room temperature were tested.

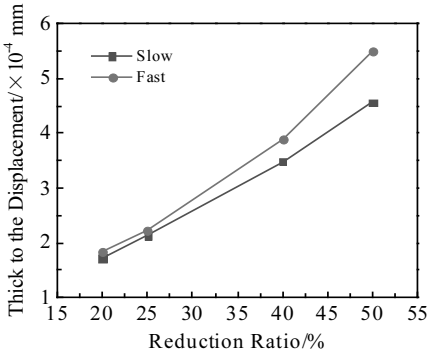

Fig.6 Variation curves of plate thickness displacement with rolling reductions

AZ31B magnesium alloy plate was used in the experiment, and its chemical composition is shown in Table 3. The initial state of the plate is annealing, with a thickness of 2 mm. Before rolling, the plate is cut into a 200 mm×50 mm rectangle by wire cutting method and heated to 280 ºC by heating furnace. The rolling mill used for rolling is a magnesium alloy six-roller high temperature mill independently designed by Liaoning University of Science and Technology.

The tensile test was conducted in accordance with the national standard GB/T228-2002 “tensile test methods for metallic materials at room temperature”, and the tensile test samples were prepared in consideration of actual experimental conditions. In order to consider the inhomogeneity of the sample and the accidental error of the instrument, we use the arithmetic mean value method of multi-point measurement to process the data when measuring the microhardness.

2.2 Analysis of experimental results

2.2.1 Metallographic microstructure evolution of magnesium alloy plate

The structure changes in the rolling direction (RD) are shown in Fig.8. Fig.8a is the initial slab with a thickness of 2 mm. Fig.8b~8e indicate the microstructures that are placed in the air for natural cooling after rolling with the reduction rate of 20%, 25%, 40% and 60% respectively, that is, the reduction of 0.4, 0.5, 0.8 and 1.2 mm. Fig.8b′~8e′ indicate the microstructures that are quickly put into water for cooling after rolling. As can be seen from the figure, after the magnesium alloy plate is warm-rolled, the grain in the rolling direction (RD) changes significantly, i.e. the grain is stretched along the rolling direction to some extent, and the grain is refined.

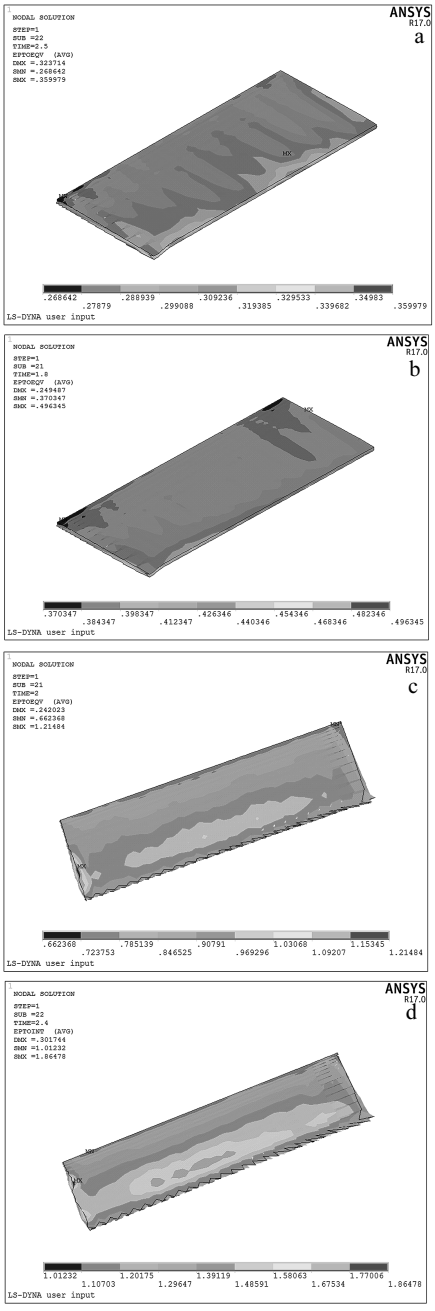

Fig.7 Cloud diagram of equivalent strain distribution of plate fully rolled under different rolling reductions: (a) 0.4 mm, (b) 0.5 mm, (c) 0.8 mm, and (d) 1.0 mm

And with the increase of the rolling reduction, the elongation has a certain extent of expansion. When the reduction is 0.4 and 0.5 mm, that is, Fig.8b, 8b′, 8c, 8c′, although there is grain refinement, some grains are still large in size, and the grain size is very uneven. When the reduction increases to 0.8 mm, that is, Fig.8d and 8d′, the grain size is relatively uniform, the grain size further decreases, and the number of large grains decreases sharply. When the reduction continues to increase to 1.2 mm, that is, Fig.8e and 8e′, the grain refinement shows good uniformity, and the large grain is hardly observed. The above indicates that the rolling reduction has a great influence on the grain refinement of AZ31B magnesium alloy, and with the increase of the reduction, the smaller the grain, the more uniform the grain refinement.

Table 3 Chemical composition of AZ31B magnesium alloy plate (wt%)

Al	Si	Ca	Zn	Mn	Cu	Mg
3.2	0.07	0.04	1.2	0.8	0.01	94.68

It can also be seen from the horizontal comparison in the figure that the cooling mode of AZ31B magnesium alloy plate after warm rolling also has a great influence on its microstructure. Compared with the natural cooling in air after rolling and the rapid cooling in water, it is found that the natural cooling in air is more likely to produce grain refinement and the grain is more uniform, but the rapid water cooling only produces small grains. The reason is that, compared with rapid water cooling, natural cooling in air is more conducive to secondary crystallization, and the original grains have more time to produce new grains and grow up, and the grains are relatively uniform. Though rapid water cooling can also lead to the formation of new grains and the loss of internal energy, the grains cannot continue to grow, and the grains are very different.

The organizational structure changes in the width direction (TD) are as shown in Fig.9. In the figure, 0 is the initial slab with the thickness of 2 mm. Fig.9b~9e indicate the microstructures that are placed in the air for natural cooling after rolling with the reduction rate of 20%, 25%, 40%, 60%, respectively, that is, the reduction of 0.4, 0.5, 0.8 and 1.2 mm. Fig.9b′~9e′ indicate the microstructures that are quickly put into water for cooling after rolling. As can be seen from the figure, after the magnesium alloy plate is warm-rolled, the grains in width direction (TD) show different degree of grain refinement. However, the grain in the width direction (TD) has no obvious elongation, and the grain refining law is basically the same as that in the rolling direction (RD). But from the width direction, the grain refinement is more obvious.

2.2.2 Tensile properties of magnesium alloy plate at room temperature

The mechanical properties of each sample recorded in the experiment are shown in Table 4, and the broken line graph of the mechanical properties of magnesium alloy plate under different rolling reductions and cooling conditions is drawn, as shown in Fig.10.

On the contrary, the value of tensile strength under natural air cooling is less than that under rapid water cooling. By comparing the increase of tensile strength and yield

strength of magnesium alloy thin plates, it can be seen that the effect of asynchronous rolling on yield strength is higher than that on tensile strength. The yield strength increases from 105.40 to 243.25 MPa, but the tensile strength only increases from 273.30 to 310.72 MPa.

2.2.3 Analysis of hardness of magnesium alloy plate in thickness direction

The Vickers microhardness obtained in the experiment is shown in Table 5, and the broken line graph of Vickers hardness of magnesium alloy plate under different rolling reductions and cooling conditions is drawn, as shown in Fig. 11.

By observation in the figure, it can be seen that the hardness of AZ31B magnesium alloy plate increases obviously after asynchronous rolling. As can be seen from the overall trend of the line, the hardness of the rolled part increases rapidly and the speed is fast when the reduction rate is 25%, that is, before the reduction is 0.5 mm. The hardness (HV) of rapid water cooling increases from 632 to 734.3 MPa, but the hardness of natural air cooling increases from 632 to 743.8 MPa. With the increase of the reduction, the hardness of the thin plate increases slowly and tends to be stable when it is from 0.5 mm to 0.8 mm. Comparing the two cooling methods, the hardness of the thin plate under natural air-cooling condition is always higher than its value under water-cooling condition with the increase of reduction, and the increasing trend is consistent. This phenomenon was analyzed and it was concluded that the internal grain of magnesium alloy plate is refined and recrystallized by asynchronous rolling. When the reduction is small, the internal refined grains are fewer, and the grain size is not uniform. If the reduction increases, more and more grains are refined and more and more recrystallization is generated. The grain refinement is relatively uniform, so the hardness also rises to a higher level and becomes stable. By comparing the two cooling methods of rapid water cooling and natural air cooling, we find that the internal structure of magnesium alloy plate has enough time and energy for recrystallization and grain growth, which results in more uniform grain refinement and higher hardness.

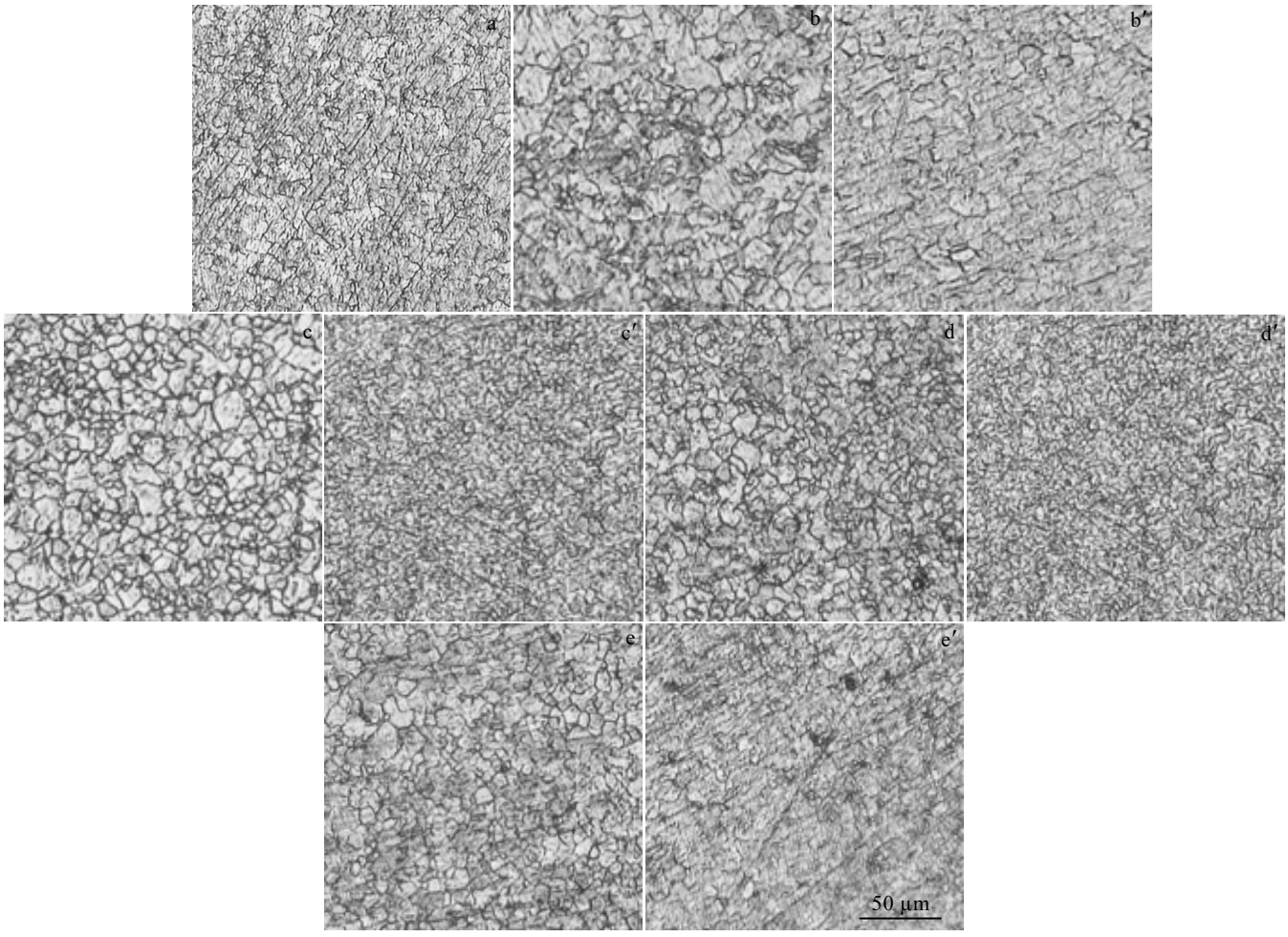

Fig.8 OM images of plate before (a) and after (b~e′) rolling with different the reduction rates in rolling direction: (b, b′) 20%, (c, c′) 25%, (d, d′) 40%, and (e, e′) 60%

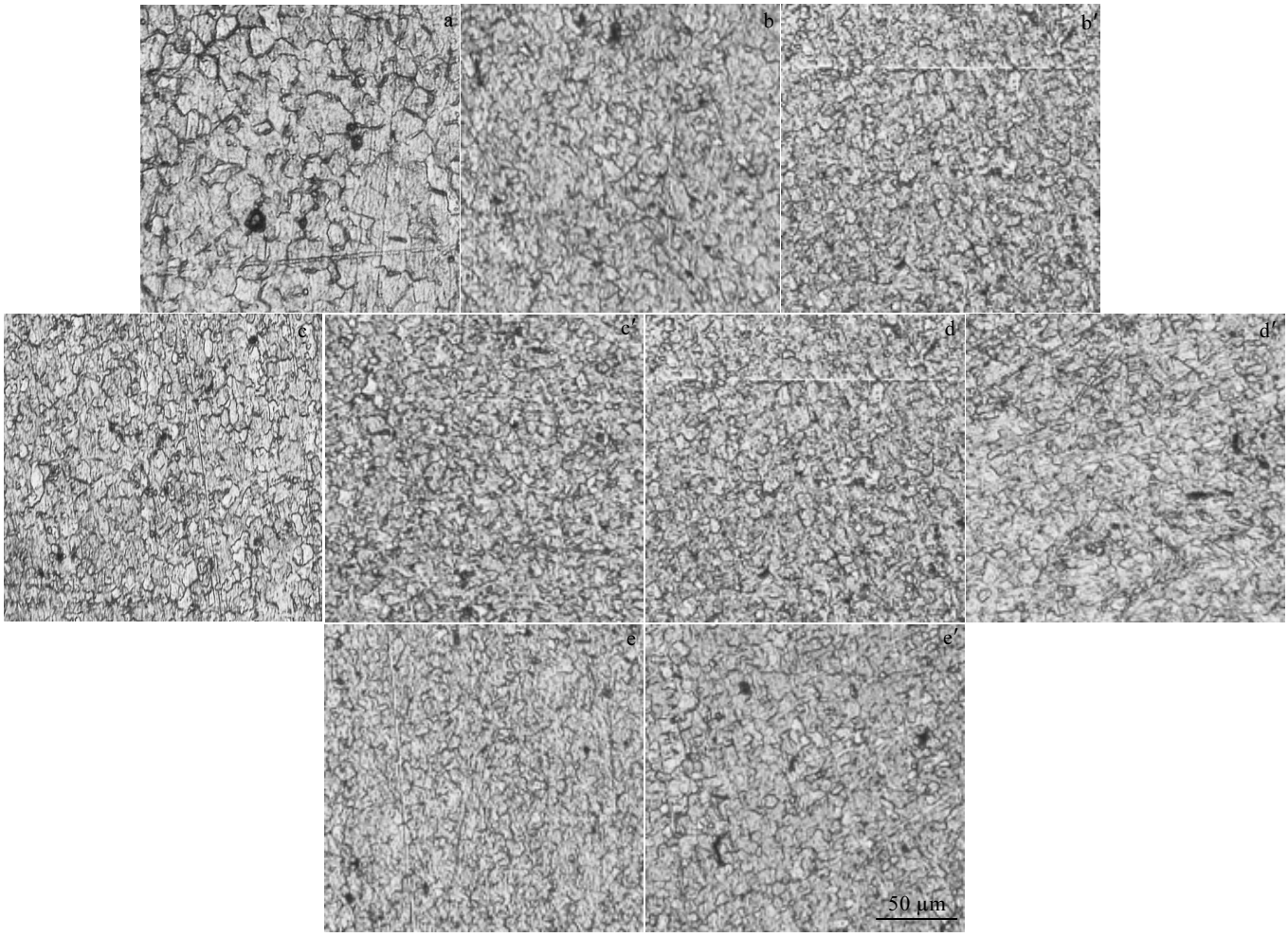

Fig.9 OM images of plate before (a) and after (b~e′) rolling with the different reduction rates in width direction: (b, b′) 20%, (c, c′) 25%, (d, d′) 40%, and (e, e′) 60%

Table 4 Uniaxial tensile property data at room temperature

Rolling reduction quantities/mm		0	0.4	0.5	0.8	1.2
Rapid water cooling	Yield strength/MPa	105.4	150.6	158.9	225.7	224.9
	Tensile strength/MPa	273.3	285.6	289.4	310.7	301.8
Natural air cooling	Yield strength/MPa	105.4	165.7	170.4	243.3	230.6
	Tensile strength/MPa	273.3	283.5	292.2	304.3	298.8

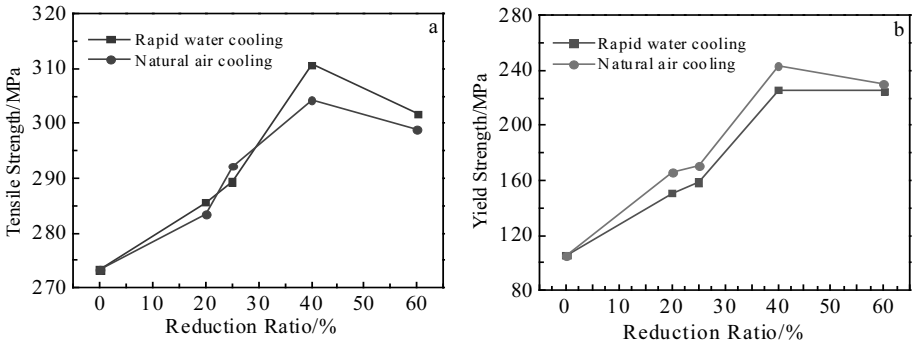

Fig.10 Variation curves of tensile strength (a) and yield strength (b) with rolling reduction ratio

Table 5 Vickers microhardness data

Rolling reduction quantities/mm	Hardness, $HV_{0.5}$/MPa	
	Quick water cooling	Natural air cooling
0	632	632
0.4	728	744
0.5	734	752
0.8	754	782
1.2	763	791

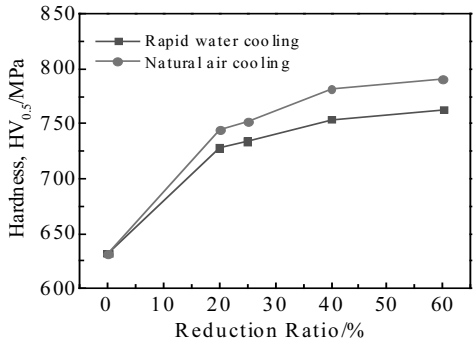

Fig.11 Variation curves of Vickers hardness with rolling reduction ratio

3 Conclusions

1) During the whole rolling process, the rolling force distribution in the head and tail of the rolled part of magnesium alloy plate is uneven, and the rolling force on the edge also varies greatly. The equivalent stress is also most concentrated in the head, tail and edge of the plate, and the edge is the most prone to plate thinning.

2) The reduction has a significant impact on the rolling force and stress concentration of the rolled part. For asynchronous rolling, the stress of the rolled part decreases from the side of the fast roll to the side of the slow roll, and the decrease rate increases with the increase of the reduction. In addition, the reduction has a great influence on the edge deformation of the rolled part. The transverse flow of the edge metal will increase significantly with the increase of the reduction. The larger the reduction is, the greater the edge deformation will be.

3) After asynchronous rolling at 280 °C, the internal microstructure changes, and the internal grains are refined and recrystallized. With the increase of rolling reduction, the internal grains recrystallize more and more evenly.

4) After asynchronous rolling, the mechanical properties of the magnesium alloy plate are improved and show certain rules with the increase of the reduction. The tensile strength increases from 273.3 to about 300 MPa, the yield limit increases from 105.4 to about 225 MPa, and the surface hardness (HV) also increases from 632 to about 780 MPa.

5) The research results of this paper have certain reference value for the study of microstructure, stress and strain analysis, shape design and development of warm-rolled magnesium alloy plate products.

References

1 Pei Daoding, Bin Jiang, Jian Wang *et al*. *Materials Science Forum*[J], 2007, 546-549: 361
2 Xian Luo, Tan Qiyang, Mo Ning *et al*. *Transactions of Nonferrous Metals Society of China*[J], 2019, 29(7): 1424
3 Schumann S, Friedrich H. *Materials Science Forum*[J], 2003, 419-422: 51
4 Duan Yali, Zhang Zhimin, Xue Yong. *Hunan Nonferrous Metals*[J], 2007(1): 38 (in Chinese)
5 Dziubinska A, Gontarz A. *Aircraft Engineering and Aerospace Technology*[J], 2016, 88(3): 452
6 Zheng Hongxia, Li Baokuan, Chang Zezhou. *Steelmaking*[J], 2001(2): 20
7 Zhai Qiuya, Wang Zhimin, Yuan Sen *et al. Journal of Xi'an University of Technology*[J], 2002(3): 254 (in Chinese)
8 Gao Xiangyu, Huang Qingxue, Zhu Lin *et al*. *Hot Working Technology*[J], 2017, 46(21): 90 (in Chinese)
9 Mu Shengbin. *World Nonferrous Metals*[J], 2016(12): 41 (in Chinese)
10 Pang Linghuan, Xu Chun, Chen Qizhong. *Shanghai Metal*[J], 2018, 40(6): 79 (in Chinese)
11 Liu Zheng, Zhang Kui, Zeng Xiaoqin. *Theoretical Basis and Application of Magnesium Based Light Alloy*[M]. Beijing: China Machine Press, 2002 (in Chinese)
12 Zhan Meiyan, Li Yuanyuan, Chen Wande *et al*. *Journal of South China University of Technology: Natural Science Edition*[J], 2007, 35(8): 16 (in Chinese)
13 Kobayashi H, Watari H. *Defect and Diffusion Forum*[J], 2019, 394: 55
14 Chen Qiang, Lin Jun, Shu, Dayu *et al*. *Materials Science and Engineering A*[J], 2012, 554: 129
15 Hwang Y M, Wang Y L. *Key Engineering Materials*[J], 2019, 794: 113
16 Huang Zhiquan, Wei Jianchun, Huang Qingxue *et al*. *Rare Metal Materials and Engineering*[J], 2018, 47(10): 2942
17 Shen Yuteng. *Effect of Differential Speed Rolling Process On Microstructure of AZ31 Magnesium Alloy Sheet*[D]. Chongqing: Chongqing University, 2016 (in Chinese)
18 Zhou L, Huang Z Y, Wang C Z *et al. Mechanics of Materials*[J], 2016, 93: 32 (in Chinese)
19 Wang Tao. *Experimental and Numerical Study on Constrained Groove Pressing of AZ31B Magnesium Alloy*[D]. Jinan: Shandong University, 2018 (in Chinese)
20 Zhao Lingjie, Zhang Chi, Wang Shun *et al. Journal of Netshape Forming Engineering*[J], 2015, 7(4): 62 (in Chinese)
21 Shen Lulu, Cao Xiaoqing, Liu Wenzheng. *Hot Working Technology*[J], 2016, 45(1): 96 (in Chinese)

22 Ren Yifang, Lan Yongting, Chen Yuan *et al*. *Journal of Guangxi University of Science and Technology*[J], 2018, 29(3): 43 (in Chinese)
23 Wang Zepeng, Hu Renxi, Kang Shiting *et al*. *Example tutorial of ANSYS 13.0/LS-DYNA Nonlinear Finite Element Analysis*[M]. Beijing: China Machine Press, 2011 (in Chinese)
24 Ou Xinran. *Finite Element Simulation of Asynchronous Rolling Process of Magnesium Alloy Plate*[D]. Chongqing: Chongqing University, 2015 (in Chinese)
25 Guo Lili, Wang Changfeng, Zhan Jian. *Journal of Plasticity Engineering*[J], 2017, 24(6): 48 (in Chinese)
26 Ginzberg V B. Ma Dongqing *et al*. *Plate and Strip Rolling Technology*[M]. Beijing: Metallurgical Industry Press, 1998 (in Chinese)
27 Nene S, Kashyap B P, Prabhu N *et al*. *Advanced Materials Research*[J], 2014, 922: 537
28 Zheng Xuanxuan. *Finite Element Simulation and Experimental Research on Rolling Process of AZ31 Magnesium Alloy Plate* [D]. Zhenjiang: Jiangsu University, 2018 (in Chinese)
29 Gong Feng, Zhang Shun, Wu Tingdao. *Journal of Mechanical Engineering*[J], 2014, 50(24): 44 (in Chinese)
30 Wang Chengguo, Lin Lijing, Liu Hongli *et al. Journal of Netshape Forming Engineering*[J], 2012, 4(6): 82 (in Chinese)
31 Huang Biao, Yan Hongge, Chen Jihua *et al*. *Materials for Mechanical Engineering*[J], 2018, 42(6): 69 (in Chinese)

镁合金薄板异步轧制的数值模拟与实验研究

汪　曦，薛政坤，于晓光，杨有泽
(辽宁科技大学 机械工程与自动化学院，辽宁 鞍山 114051)

摘　要：采用数值模拟技术和实验研究，分析了不同工艺参数对镁合金薄板单向异步轧制产品性能的影响规律。运用ANSYS/LS-DYNA 有限元软件完成了数值模拟，进行了不同轧制条件下的单向异步轧制实验研究。利用金相显微镜观察了内部组织结构，采用拉伸试验机和显微维氏硬度仪等实验手段，检测了镁合金薄板的屈服强度、抗拉伸强度及硬度等力学性能。

关键词：镁合金薄板；异步轧制；数值模拟；金相显微组织；单向拉伸

作者简介：汪　曦，女，1964 年生，硕士，副教授，辽宁科技大学机械工程与自动化学院，　辽宁　鞍山　114051，　E-mail: wx1870@yeah.net